Comparison of cosmological models using recent supernova data

S. Nesseris and L. Perivolaropoulos*

Department of Physics, University of Ioannina, 45110 Ioannina, Greece
(Received 26 January 2004; published 24 August 2004)

We study the expansion history of the universe up to a redshift of z=1.75 using the 194 recently published SnIa data by Tonry *et al.* and Barris *et al.* In particular we find the best fit forms of several cosmological models and $H(z)$ ansatze, determine the best fit values of their parameters and rank them according to increasing value of χ^2_{min} [the minimum value of χ^2 for each $H(z)$ ansatz]. We treat Ω_{0m} as a parameter using a reasonable prior and assume flat geometry of the universe. No prior assumptions are made about validity of energy conditions. The fitted models are fourteen and include standard cold dark matter (SCDM), cold dark matter with cosmological constant Λ (LCDM), dark energy with constant equation of state parameter w (quiessence), third order polynomial for $H(1+z)$, Chaplygin gas, Cardassian model, $w(z)=w_0+w_1 z$, $w(z)=w_0+zw_1/(1+z)$, an oscillating ansatz for $H(z)$, etc. All these models with the exception of SCDM are consistent with the present data. However, the quality of the fit differs significantly among them and so do the predicted forms of $w(z)$ and $H(z)$ at best fit. The worst fit among the data-consistent models considered corresponds to the simplest model LCDM ($\chi^2_{min}=198.7$ for $\Omega_{0m}=0.34$) while the best fit is achieved by the three parameter oscillating ansatz ($\chi^2_{min}=193.8$). Most of the best fit ansatze have an equation of state parameter $w(z)$ that varies between $w(z)\simeq-1$ for $z<0.5$ to $w(z)>0$ for $z>1$. This implies that the sign of the pressure of the dark energy may be alternating as the redshift increases. The goodness of fit of the oscillating $H(z)$ ansatz lends further support to this possibility.

I. INTRODUCTION

One of the fundamental goals of cosmology is the understanding of the global history of the Universe. Using objects of approximately known absolute luminocity (standard candles) in the nearby universe provides the current rate of expansion. Using more distant standard candles like type Ia supernovae (SnIa) makes it possible to start seeing the varied effects of the Universe's expansion history. Such cosmological observations have indicated [1] that the Universe undergoes accelerated expansion during recent redshift times. This accelerating expansion has been attributed to a dark energy component with negative pressure which can induce repulsive gravity and thus cause accelerated expansion. The simplest and most obvious candidate for this dark energy [2] is the cosmological constant [3] with equation of state $w=p/\rho=-1$.

The extremely fine tuned value of the cosmological constant required to induce the observed accelerated expansion has led to a variety of alternative models where the dark energy component varies with time. Many of these models make use of a homogeneous, time dependent minimally coupled scalar field ϕ (quintessence [4,5]) whose dynamics is determined by a specially designed potential $V(\phi)$ inducing the appropriate time dependence of the field equation of state $w(z)=p(\phi)/\rho(\phi)$. Given the observed $w(z)$, the quintessence potential can in principle be determined. Other physically motivated models predicting late accelerated expansion include modified gravity [6–8], Chaplygin gas [9], Cardassian cosmology [10], theories with compactified extra dimensions [11,12], braneworld models [13], etc. Such cos-

mological models predict specific forms of the Hubble parameter $H(z)$ as a function of redshift z in terms of arbitrary parameters. These parameters are determined by fitting to the observed luminocity distance $d_L(z)$ using the relation [14–16] (valid in a flat universe)

$$H(z)=c\left[\frac{d}{dz}\left(\frac{d_L(z)}{1+z}\right)\right]^{-1}. \qquad (1.1)$$

This is easily derived using the relation between $d_L(z)$ and the comoving distance $r(z)$ (where z is the redshift of light emission)

$$d_L(z)=r(z)(1+z) \qquad (1.2)$$

and the light ray geodesic equation in a flat universe $cdt=a(z)dr(z)$ where $a(z)$ is the scale factor.

Another similar approach towards determining the expansion history $H(z)$ is to assume an arbitrary ansatz for $H(z)$ which is not necessarily physically motivated (it is "model independent") but is specially designed to give a good fit to the data for $d_L(z)$. Given a particular cosmological model (or ansatz) for $H(z;a_1,\ldots,a_n)$ where $a_1,\ldots,a_n$ are model parameters, the maximum likelihood technique can be used to determine the best fit values of parameters (with $1\sigma-2\sigma$ errors) as well as the goodness of the fit of the ansatz to the data. This technique can be summarized as follows: The observational data consist of N apparent magnitudes $m_i(z_i)$ and redshifts z_i with their corresponding errors δm_i and δz_i. Each apparent magnitude is related to the corresponding luminocity distance d_L of the SnIa by

$$m(z)=M+5\log_{10}\left[\frac{d_L(z)}{\text{Mpc}}\right]+25, \qquad (1.3)$$

*Electronic address: http://leandros.physics.uoi.gr

where M is the absolute magnitude which is assumed to be constant for standard candles like Type Ia SnIa. From Eqs. (1.1) and (1.3) it becomes clear that the luminocity distance $d_L(z)$ is the "meeting point" between the observed apparent magnitude $m(z)$ and the theoretical prediction $H(z)$.

The apparent magnitude can also be expressed in terms of the dimensionless "Hubble-constant free" luminocity distance D_L defined by

$$D_L(z) = \frac{H_0 d_L(z)}{c} \qquad (1.4)$$

as

$$m(z) = \bar{M}(M, H_0) + 5\log_{10}(D_L(z)), \qquad (1.5)$$

where $\bar{M}$ is the magnitude zero point offset and depends on M and H_0 as

$$\bar{M} = M + 5\log_{10}\left(\frac{c/H_0}{1\ \text{Mpc}}\right) + 25. \qquad (1.6)$$

The zero point offset is an additional model independent parameter that needs to be fit along with the model parameters $a_1, \ldots, a_n$. However, since $\bar{M}$ is model independent its value from a specific good fit can be used directly to other fits of model parameters. Thus the observed $m_i(z_i)$ can be translated to $D_{Li}^{obs}(z_i)$ using Eq. (1.5) for the best fit value of $\bar{M}_{obs}$ obtained from nearby SnIa. The theoretically predicted value $D_L^{th}(z)$ in the context of a given model $H(z; a_1, \ldots, a_n)$ can be obtained by integrating Eq. (1.1) as

$$D_L^{th}(z) = (1+z)\int_0^z dz' \frac{H_0}{H(z'; a_1, \ldots, a_n)}. \qquad (1.7)$$

The best fit values for the parameters $a_1, \ldots, a_n$ are found by minimizing the quantity

$$\chi^2(a_1, \ldots, a_n) = \sum_{i=1}^N \frac{(\log_{10}D_L^{obs}(z_i) - \log_{10}D_L^{th}(z_i))^2}{(\sigma_{\log_{10}D_L(z_i)})^2 + \left(\frac{\partial\log_{10}D_L(z_i)}{\partial z_i}\sigma_{z_i}\right)^2}, \qquad (1.8)$$

where σ_z is the 1σ redshift uncertainty of the data and $\sigma_{\log_{10}D_L(z_i)}$ is the corresponding 1σ error of $\log_{10}D_L^{obs}(z_i)$.

The probability distribution for the parameters $a_1, \ldots, a_n$ is [17]

$$P(a_1, \ldots, a_n) = \mathcal{N}e^{-\chi^2(a_1, \ldots, a_n)/2}, \qquad (1.9)$$

where $\mathcal{N}$ is a normalization constant. If prior information is known on some of the parameters $a_1, \ldots, a_n$, then we can either fix the known parameters using the prior information or "marginalize," i.e., average the probability distribution (1.9) around the known value of the parameters with an appropriate "prior" probability distribution. Here we use the former approach (fix the parameters with prior information) for simplicity. This simplification has negligible effect on our results as it can be verified by comparing some of our results

with corresponding results in the literature where marginalization has been used [e.g., Ref. [18] for cold dark matter with cosmological constant Λ (LCDM)].

It is straightforward to minimize $\chi^2(a_1, \ldots, a_n)$ using numerical libraries like NAG [19,20] (see also Ref. [17]) or packages like Mathematica [21] to find $\chi^2_{min}(\bar{a}_1, \ldots, \bar{a}_n)$ [22] where χ^2_{min} is the minimum obtained for the best fit parameter values $\bar{a}_1, \ldots, \bar{a}_n$. If $\chi^2_{min}/(N-n) \lesssim 1$ the fit is good and the data are consistent with the considered model $H(z; a_1, \ldots, a_n)$.

The variable χ^2_{min} is random in the sense that it depends on the random data set used. Its probability distribution is a χ^2 distribution for $N-n$ degrees of freedom [17]. This implies that 68% of the random data sets will give a χ^2 such that

$$\chi^2(a_1, \ldots, a_n) - \chi^2(\bar{a}_1, \ldots, \bar{a}_n) \leq \Delta\chi^2_{1\sigma}(n), \quad (1.10)$$

where $\Delta\chi^2_{1\sigma}(n)$ is 1 for $n=1$, 2.3 for $n=2$, 3.53 for $n=3$, etc. Thus Eq. (1.10) defines closed ellipsoidal surfaces around $\bar{a}_1, \ldots, \bar{a}_n$ in the n dimensional parameter space. The corresponding 1σ range of the parameter a_i is the range of a_i for points contained within this ellipsoidal surface. Similarly, it can be shown that 95.4% of the random data sets will give a χ^2 such that

$$\chi^2(a_1, \ldots, a_n) - \chi^2(\bar{a}_1, \ldots, \bar{a}_n) \leq \Delta\chi^2_{2\sigma}(n), \quad (1.11)$$

where $\Delta\chi^2_{2\sigma}(n)$ is 4.0 for $n=1$, 6.17 for $n=2$, 8.02 for $n=3$, etc. Thus Eq. (1.11) defines the 2σ ellipsoidal surface in parameter space and similarly for higher σ's.

II. COSMIC EXPANSION HISTORY

We now apply the above described maximum likelihood method using a recently published data set consisting of 194 ($N=194$) SnIa [23,24]. This is a subset of the total of 253 published SnIa sample obtained by imposing constraints $A_V < 0.5$ (excluding high extinction) and $z > 0.01$ (reducing peculiar velocity effects). Each data point at redshift z includes the logarithm of the Hubble-free luminocity distance $\log_{10}[cD_L^{obs}(z)]$ and the corresponding error $\sigma_{\log_{10}D_L(z)}$. A table of the data we used can be downloaded in electronic form [22]. These Hubble-free luminosity distances are obtained assuming a best fit value for the zero point magnitude offset $\bar{M}$ [18]. We adopt this same value for $\bar{M}$ and choose not to treat $\bar{M}$ as an additional free parameter to fit (and marginalize) along with the parameters of each theoretical model studied. In the Appendix we demonstrate that marginalization over $\bar{M}$ would have negligible effect [$O(1\%)$] on our results. Also, comparison of our results for LCDM and quiessence [$w(z) = $constant] with the corresponding results of Ref. [18] where marginalization of $\bar{M}$ was implemented indicates that our simplified approach has negligible effect on the obtained results. This same conclusion has also been reached in Ref. [25] and it's origin is demonstrated in the Appendix.

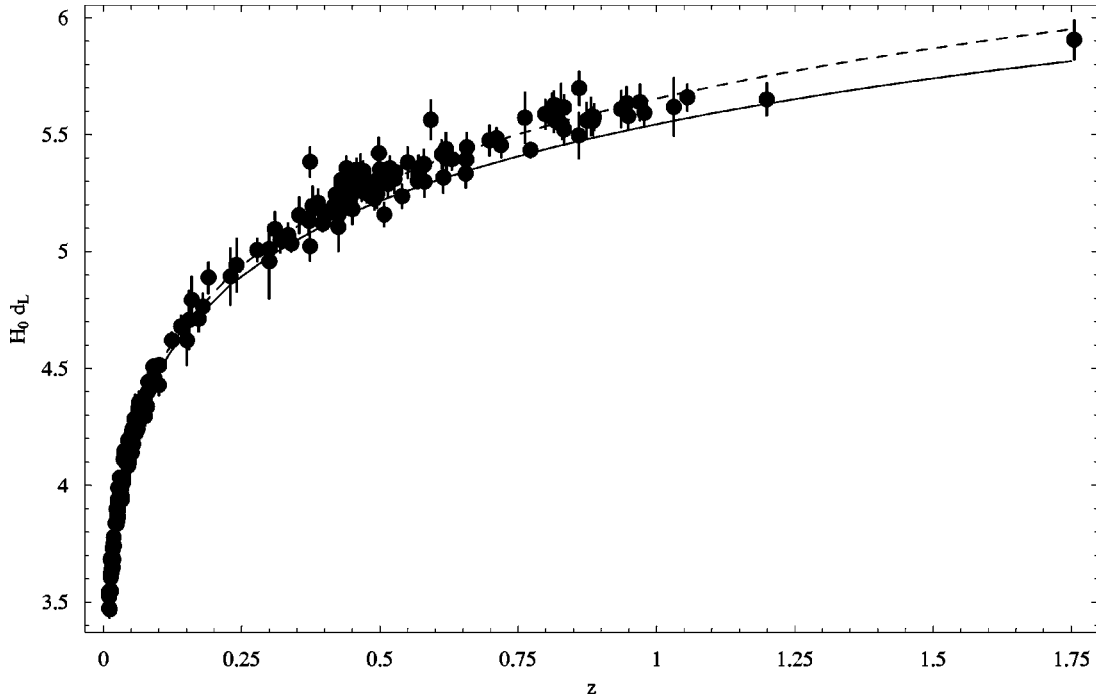In the construction of χ^2 using Eq. (1.8) we have used a

FIG. 1. The observed 194 SnIa Hubble free luminocity distances along with the theoretically predicted curves in the context of SCDM (continuous line) and LCDM (dashed line).

value of σ_z corresponding to uncertainties due to peculiar velocities with $\Delta v = \Delta(cz) = 500$ km/s which implies $\sigma_z = \Delta z = (500$ km/s$)/c$. The minimization of Eq. (1.8) was implemented for each theoretical model using a simple Mathematica code which can be downloaded along with the table of the data set used [22] (or can be sent by e-mail upon request).

We now proceed to apply likelihood testing to various theoretical models. Each model is defined by its predicted Hubble-parameter $H(z)$. For example for LCDM we have

$$H^2(z;\Omega_{0m}) = \left(\frac{\dot{a}}{a}\right)^2 = H_0^2[\Omega_{0m}(1+z)^3 + (1-\Omega_{0m})]$$

$$(2.1)$$

and there is a single parameter Ω_{0m} to be fit from the data. The simplest model to consider however is standard cold dark matter (SCDM) defined by

$$H^2(z) = H_0^2(1+z)^3 \qquad (2.2)$$

with no free parameters. Using Eq. (2.2) in Eq. (1.7) we calculate $D_L^{th}(z)$. We may then find χ^2 using Eq. (1.8) and minimize to find χ^2_{min}. In the SCDM case there are no free parameters to vary and no minimization is needed. We thus find $\chi^2 = \chi^2_{min} = 431.4$, which implies $\chi^2_{min}/\text{dof} = 2.2$ (dof = degrees of freedom). Since this value χ^2_{min}/dof is significantly larger than 1 we conclude that SCDM does not provide a good fit to the SnIa data.

The next simplest model consistent with the flatness indicated by WMAP [26] is LCDM defined by Eq. (2.1). It is straightforward to evaluate $D_L^{th}(z)$ numerically [using Eq.

(2.1) in Eq. (1.7)] and use it to evaluate $\chi^2(\Omega_{0m})$ from Eq. (1.8). A minimization of this expression leads to [22]

$$\chi^2_{min} = \chi^2(\Omega_{0m} = 0.34) = 198.74, \qquad (2.3)$$

which implies $\chi^2/\text{dof} = 1.03$ (dof = 194 − 1 = 193). This model is clearly consistent with the data since $\chi^2/\text{dof} \simeq 1$. The 1σ errors on the predicted value of $\Omega_{0m} = 0.34$ are found by solving the equation

$$\chi^2(\Omega_{m1\sigma}) - \chi^2_{min} = \Delta\chi^2_{1\sigma}(n=1) = 1 \qquad (2.4)$$

which leads to

$$\Omega_{0m} = 0.34 \pm 0.032. \qquad (2.5)$$

This result is identical with the result of Ref. [18] even though our 1σ errors are slightly smaller.

In Fig. 1 we show a comparison of the observed 194 SnIa Hubble free luminosity distances along with the theoretically predicted curves in the context of SCDM (continuous line) and LCDM (dashed line). In this case it is even visually obvious that LCDM provides a good fit to the data contrary to the case of SCDM. This visual distinction is not possible when comparing the other data-compatible models discussed below with LCDM. We thus do not attempt to include the theoretical curves corresponding to other models on the same plot.

We now consider other more general models and ansatze which, however, reduce for certain parameter values to LCDM. If these parameter values give a $\chi^2(\text{LCDM})$ that is beyond the 2σ level away from the minimum χ^2_{min}, then we would conclude that LCDM is disfavored compared to the

better fit model. Even if we just find models with $\chi^2_{min} < \chi^2_{min}(\text{LCDM}) = 198.74$ but within 1σ we still have useful information since these models are more probable than LCDM.

We start with a simple generalization of LCDM: We replace the cosmological constant energy density by a dark energy with constant equation of state parameter. This ansatz has been called "quiessence" in the literature [27]. The form of $H(z)$ is

$$H^2(z;\Omega_{0m},w) = H_0^2[(\Omega_{0m}(1+z)^3 + (1-\Omega_{0m})(1+z)^{3(1+w)}]. \quad (2.6)$$

This ansatz has two free parameters Ω_{0m} and w. We use prior information from large scale structure ($\Omega_{0m}h = 0.2 \pm 0.03$ [28] with $h = 0.72 \pm 0.08$ [29]) to vary Ω_{0m} in the range $\Omega_{0m} = 0.29 \pm 0.05$ in this and in all subsequent ansatze. We thus evaluate $\chi^2(w)$ and minimize with respect to w and Ω_{0m}. We find

$$\chi^2_{min} = \chi^2(w = -1.01, \Omega_{0m} = 0.34) = 198.69. \quad (2.7)$$

Including the 1σ errors we have

$$w = -1.01 \pm 0.08 \quad (2.8)$$

which is identical with the corresponding result of Ref. [18]. Thus, the minimization of this generalized ansatz gives a best fit that is indistinguishable at the 1σ level from LCDM. This means either that LCDM is truly the best fit model or that we have not chosen a general enough ansatz to see a better fit.

A further generalized ansatz involves the combination of cosmological constant with quiessence (quiessence-Λ ansatz).

The form of $H(z)$ in this case is

$$H^2(z;a_1,w_1) = H_0^2[\Omega_{0m}(1+z)^3 + a_1(1+z)^{3(1+w_1)} + (1-\Omega_{0m}-a_1)]. \quad (2.9)$$

Minimizing $\chi^2(a_1,w_1,\Omega_{0m})$ with respect to w_1, a_1, Ω_{0m} we find

$$\chi^2_{min} = \chi^2(w_1 = 2.36, \ a_1 = (5 \ 10^{-3}),$$
$$\Omega_{0m} = 0.24) = 195.1. \quad (2.10)$$

Including the error bars we have

$$w_1 = 2.36^{+0.44}_{-0.78}, \ a_1 \simeq (5 \ ^{+0.4}_{-0.9})10^{-3}. \quad (2.11)$$

Clearly the fit is better compared to LCDM but the $\chi^2(\text{LCDM}) = \chi^2(a_1 = 0, \Omega_{0m} = 0.34) = 198.7$ corresponding to LCDM with $\Omega_{0m} = 0.34$ differs by less than $\Delta\chi^2_{2\sigma}(n=2) = 6.17$ from χ^2_{min}. Therefore, LCDM is consistent at the 2σ level (but not at the 1σ) with the best fit of this ansatz. Nevertheless, given that this fit is better it is interesting to compare the dark energy properties corresponding to this ansatz at best fit with those of LCDM. These properties are well described by the effective equation of state parameter

$w(z) = p(z)/\rho(z)$ which in general (and in this case) depends on the redshift z. We can express $w(z)$ in terms of $H(z)$, dH/dz, and Ω_{0m} using the Friedman equations

$$H^2 = \frac{\dot{a}^2}{a^2} = \frac{8\pi G}{3}(\rho_m + \rho_{DE}) \quad (2.12)$$

and

$$q \equiv -\frac{\ddot{a}}{aH^2} = \frac{4\pi G}{3H^2}[\rho_m + (\rho_{DE} + 3p_{DE})], \quad (2.13)$$

where q is the deceleration parameter and we have defined as dark energy any other homogeneous and isotropic source of gravity apart from matter. Using Eqs. (2.12) and (2.13) we find

$$p_{DE} = \frac{H^2}{4\pi G}\left(q - \frac{1}{2}\right). \quad (2.14)$$

Using Eqs. (2.12) and (2.14) we find [30]

$$w(z) = \frac{p_{DE}(z)}{\rho_{DE}(z)} = \frac{2q(z) - 1}{3[1 - \Omega_m(z)]}, \quad (2.15)$$

where

$$\Omega_m(z) = \frac{8\pi G\rho_m(z)}{3H^2(z)} = \Omega_{0m}(1+z)^3\frac{H_0^2}{H^2}. \quad (2.16)$$

Using now the definitions of q and H it is easy to show that

$$q = -1 + (1+z)\frac{d\ln H}{dz}. \quad (2.17)$$

Thus substituting Eq. (2.17) in Eq. (2.15) we have

$$w(z) = \frac{p_{DE}(z)}{\rho_{DE}(z)} = \frac{\frac{2}{3}(1+z)\frac{d\ln H}{dz} - 1}{1 - \left(\frac{H_0}{H}\right)^2\Omega_{0m}(1+z)^3}. \quad (2.18)$$

In the case of generalized Friedman equations valid in modified gravity models, Eq. (2.18) can still be useful in characterizing the expansion history but it should not be interpreted as a property of an energy substance. Using the best fit form of the quiessence-Λ (q-Λ) ansatz in Eq. (2.18) we find the predicted form of $w(z)$ which is plotted in Fig. 2 along with the 1σ and 2σ error regions obtained by maximal variation of the parameters a_1 and w_1 within the 1σ and 2σ error contours of χ^2 as described in the previous section. This form of $w(z)$ (without error regions) along with the corresponding forms predicted by the other ansatze discussed below, is also shown in Fig. 3. Clearly $w(z)$ differs significantly from the LCDM prediction of $w = -1$ at redshifts $z > 0.4$. In particular we find $w(z) \simeq -1$ for $z < 0.4$ while $w(z) \simeq 2$ for $z \gtrsim 1$. Thus, this ansatz gives us a hint for the "metamorphosis" of dark energy from antigravity
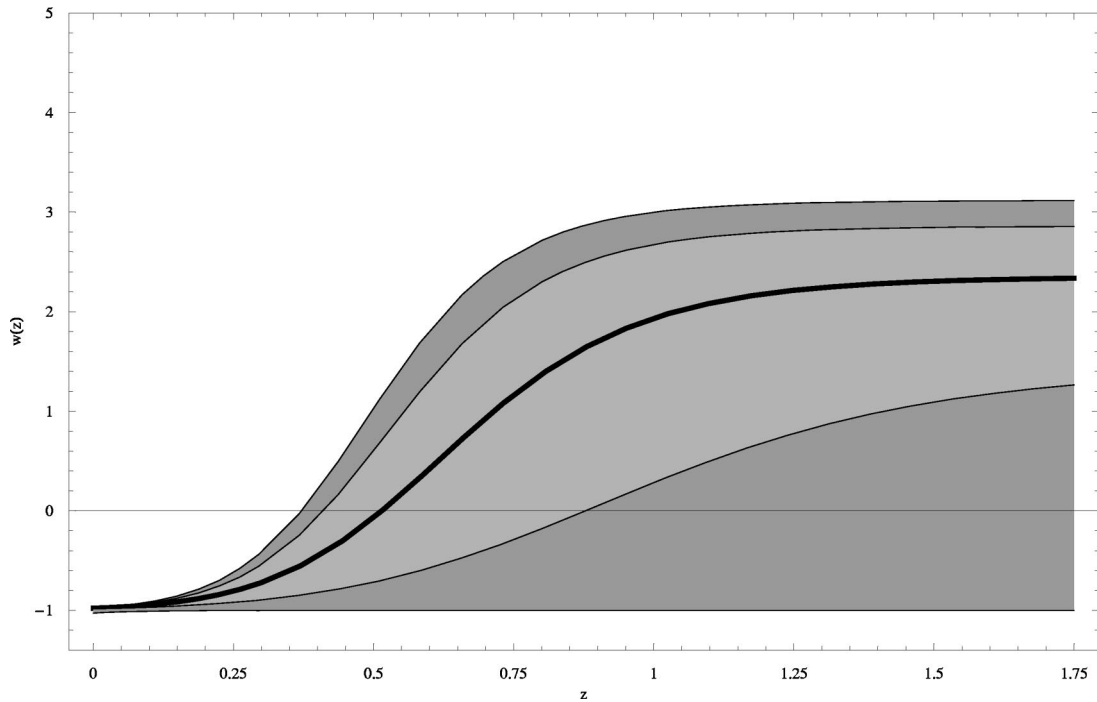
FIG. 2. The redshift dependence of the equation of state parameter $w(z)$ for the $q - \Lambda$ ansatze. The thick curve is the best fit and the light (dark) shaded regions represent the 1σ (2σ) error regions.

($w = -1$) at low redshifts to "hypergravity" ($w \simeq 2$) at high redshifts. Clearly this metamorphosis (if true) cannot persist to arbitrarily high redshifts due to constraints coming from large scale structure and nucleosynthesis. Thus, it is either not realized in nature and we have $w(z) \lesssim 0$ at all redshifts or it is part of an oscillating behavior of the dark energy equation of state parameter. This later possibility could also help resolve the coincidence problem [31,32] and is a prediction
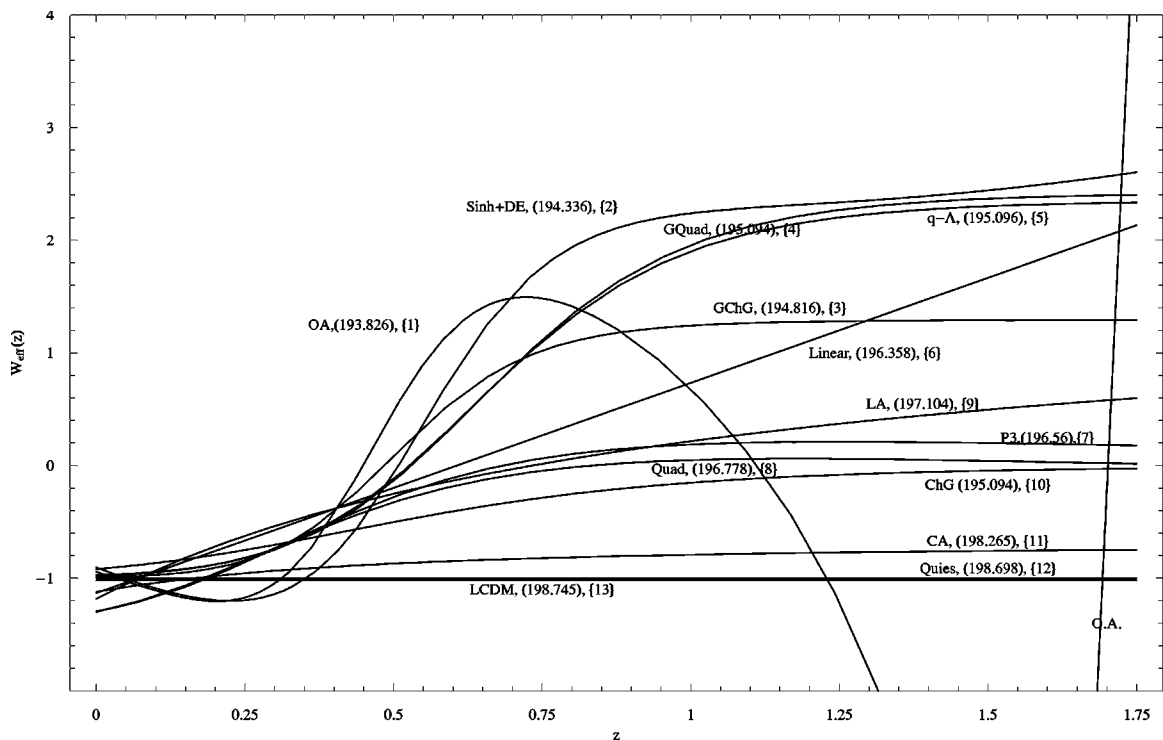

FIG. 3. The redshift dependence of the equation of state parameter for the cosmological ansatze of Table I. The numbers in the parentheses indicate the value of χ^2_{min} for each ansatz and its rank according to increasing value of χ^2_{min}. In LCDM the best fit value $\Omega_{0m} = 0.34$ was used giving $\chi^2_{min} = 198.745$.

TABLE I. Best-fit parameters.

Model	$H(z)$	χ^2_{min}	Best fit parameters
OA	$H^2(z)=H_0^2\{\Omega_{0m}(1+z)^3+a_1\cos(a_2z^2+a_3)$		$a_1=-3.22^{+0.93}_{-0.76}$, $a_2=2.28^{+0.93}_{-0.76}$
(1)	$+[1-a_1\cos(a_3)-\Omega_{0m}]\}$	193.8	$a_3=-0.08\pi\pm0.01\pi$, $\Omega_{0m}=0.34$
Sinh+DE	$H^2(z)=H_0^2[\Omega_{0m}(1+z)^3+a_1(1+z)^{3(1+w_1)}+a_2\sin h(w_2z)$		$w_1=0.19^{+0.1}_{-0.3}$, $w_2=3.66^{+0.93}_{-3.13}$
(2)	$+1-\Omega_{Om}-a_1]$	194.3	$a_1=-0.51^{+0.1}_{-0.3}$, $a_2=0.545^{+0.005}_{-0.015}$
			$\Omega_{0m}=0.32$
GCG (3)	$H^2(z)=H_0^2[\Omega_{0m}(1+z)^3+(1$	194.8	$A=0.9966^{+0.0001}_{-0.0004}$, $\alpha=13.75^{+0.02}_{-0.04}$
	$-\Omega_{0m})\sqrt{A+(1-A)(1+z)^{\alpha}}]$		
			$\Omega_{0m}=0.24$
GQ	$H^2(z)=H_0^2[\Omega_{0m}(1+z)^3+a_1(1+z)^{3(1+w_1)}$		$w_1=-1.13\pm0.24$, $w_2=2.42\pm0.02$
	$+a_2(1+z)^{3(1+w_2)}+(1-a_1-a_2-\Omega_{0m})]$		
(4)		195.1	$a_1=-57^{+3}_{-2}10^{-3}$, $a_2=4^{+0.3}_{-0.2}10^{-3}$
			$\Omega_{0m}=0.24$
q-Λ (5)	$H^2(z)=H_0^2[\Omega_{0m}(1+z)^3+a_1(1+z)^{3(1+w_1)}$	195.1	$w_1=2.36^{+0.44}_{-0.78}$, $a_1\simeq5^{+0.4}_{-0.9}10^{-3}$
	$+(1-\Omega_{0m}-a_1)]$		
			$\Omega_{0m}=0.24$
Linear	$H^2(z)=H_0^2[\Omega_{0m}(1+z)^3+(1-\Omega_{0m})$		$w_0=-1.13\pm0.09$, $w_1=1.87^{+0.08}_{-0.01}$
(6)	$\times(1+z)^{3(1+w_0-w_1)}e^{3w_1z}]$	196.4	$\Omega_{0m}=0.24$
P3	$H^2(z)=H_0^2[\Omega_{0m}(1+z)^3+a_3(1+z)^3+a_2(1+z)^2$		$a_1=-2.49\pm0.12$, $a_2=0.46^{+0.07}_{-0.05}$
(7)	$+a_1(1+z)+(1-a_1-a_2-a_3-\Omega_{0m})]$	196.6	$a_3=0.33\pm0.06$, $\Omega_{0m}=0.34$
Quad	$H^2(z)=H_0^2[\Omega_{0m}(1+z)^3+a_1(1+z)+a_2(1+z)^2$		$a_1=-3.85^{+1.16}_{-1.27}$, $a_2=1.63^{+0.79}_{-0.63}$
(8)	$+(1-a_1-a_2-\Omega_{0m})]$	196.8	$\Omega_{0m}=0.34$
LA	$H^2(z)=H_0^2[\Omega_{0m}(1+z)^3+(1-\Omega_{0m})(1+z)^{3(1+w_0+w_1)}$		$w_0=-1.18\pm0.10$, $w_1=2.79\pm0.05$
(9)	$e^{3w_1[(1/1+z)-1]}]$	197.1	$\Omega_{0m}=0.24$
CG (10)	$H^2(z)=H_0^2[\Omega_{0m}(1+z)^3+(1-\Omega_{0m})\sqrt{A+(1-A)(1+z)^6}]$	197.4	$A=0.92\pm0.03$ $\Omega_{0m}=0.24$
CA (11)	$H^2(z)=H_0^2[\Omega_{0m}(1+z)^3+(1-\Omega_{0m})f_X(z)]$	198.3	$q=45^{+8}_{-10}10^{-3}$, $n=-15^{+8}_{-9}$, $\Omega_{0m}=0.34$
QUIES (12)	$H^2(z)=H_0^2[\Omega_{0m}(1+z)^3+(1-\Omega_{0m})(1+z)^{3(1+w)}]$	198.7	$w=-1.01\pm0.08$, $\Omega_{0m}=0.34$
LCDM (13)	$H^2(z)=H_0^2[\Omega_{0m}(1+z)^3+(1-\Omega_{0m})]$	198.7	$\Omega_{0m}=0.34\pm0.03$
SCDM	$H^2(z)=H_0^2(1+z)^3$	431.4	−

[11] (see also Refs. [33,34]) of many models [35–37] with stabilized modulus [38,39] of extra dimensions.

In addition to $w(z)$ we also plot the reduced form of $H(z)$ compared to LCDM defined as

$$H_r^2(z)=\frac{H^2(z)-H^2_{LCDM}(z)}{H_0^2},\qquad(2.19)$$

where $H^2_{LCDM}\equiv0.3(1+z)^2+0.7$. The reduced best fit $H_r^2(z)$ for the q-Λ ansatz is shown in Fig. 4 along with the best fit $H_r(z)$ functions corresponding to some of the other ansatze discussed below. Even though both ansatze (q-Λ and LCDM) are consistent with the data and with each other at the 2σ level, the predicted forms of $H_r(z)$ and $w(z)$ differ significantly at $z>0.5$.

In order to shed more light to the dark energy metamorphosis puzzle we now consider more general forms of $H(z)$ ansatze. For each ansatz we identify the predicted form of $H(z)$ and the parameters requiring fitting. Then we evaluate and minimize χ^2 with respect to these parameters varying Ω_{0m} in the range $\Omega_{0m}=0.29\pm0.05$. Finally, we identify the best fit parameter values and the corresponding χ^2_{min} (see Table I), plot the corresponding $w(z)$ and $H(z)$ (see Figs. 3

and 4), and classify the models according to the goodness of fit. This classification will lead to some interesting conclusions about the generic properties of dark energy. The 1σ and 2σ regions of the $w(z)$ and $H(z)$ curves in the context of a particular ansatz are not particularly useful since other ansatze with equally good fits can give $w(z)$ and $H(z)$ best fits that are well outside the 2σ regions of the initial ansatz especially in regions with $z>1$ where just a few data points are available. Thus, in order to simplify the plots of Figs. 3 and 4 and avoid confusion we only show the best fit curves without the corresponding 1σ and 2σ regions.

We now briefly describe each one of the ansatze considered:

(1) Cubic Polynomial in $(1+z)$ (P3):

$$H^2(z)=H_0^2[\Omega_{0m}(1+z)^3+a_3(1+z)^3+a_2(1+z)^2$$
$$+a_1(1+z)+(1-a_1-a_2-a_3-\Omega_{0m})],$$
$$(2.20)$$

where a_1,a_2,a_3 are unknown parameters to be fit. The only priors used in this (and the other ansatze discussed here) are flatness and $\Omega_{0m}=0.29\pm0.05$. In contrast to Ref. [40] we have not fixed $a_3=0$ since large scale structure data do not
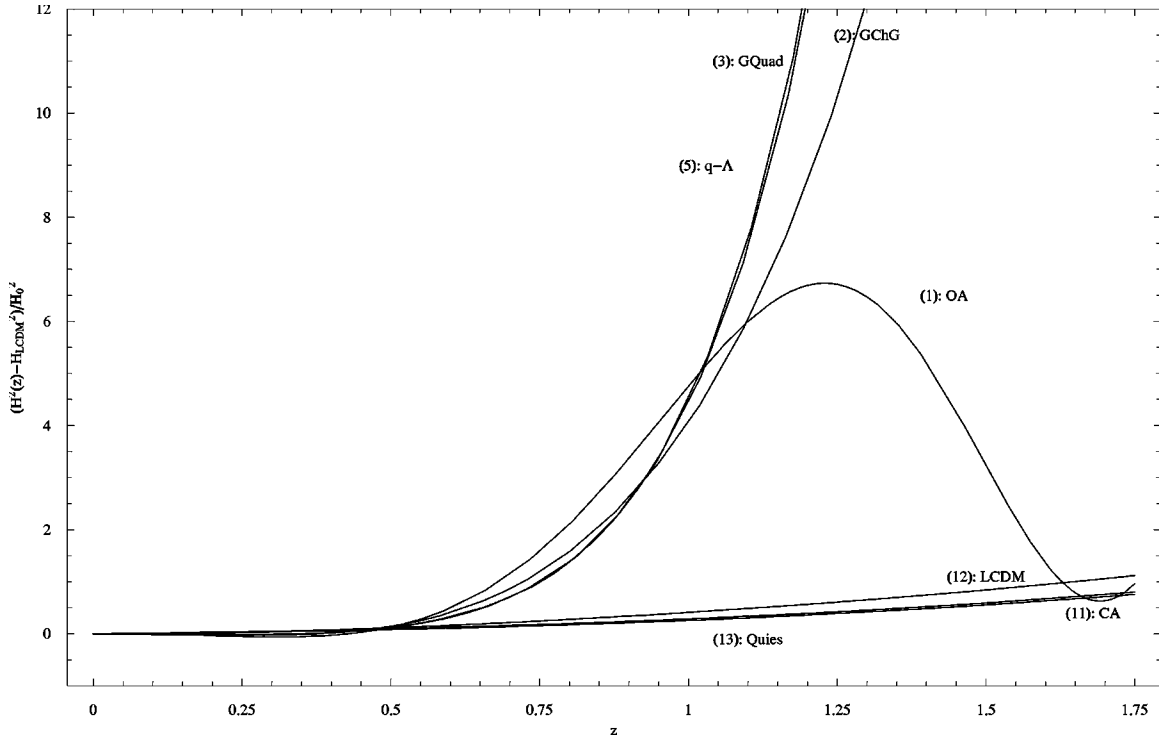
FIG. 4. The reduced Hubble parameter for some of the best and the worst fits of the cosmological ansatze of Table I. The number in the parenthesis shows the rank $(1-13)$ of the corresponding ansatz in terms of goodness of fit. The LCDM curve is not flat at zero because in its construction we used the best fit value $\Omega_{0m}=0.34$ while the H_{LCDM} on the axis assumes the prior $\Omega_{0m}=0.30$.

exclude a nonclustering form of matter with properties similar to those of hot dark matter with very large free streaming (or Jeans) length. This model has a slightly worse fit ($\chi^2_{min}=196.56$), for $\Omega_{0m}=0.34$, compared to q-Λ ($\chi^2_{min}=195.1$) but it also corresponds to $w(z)\simeq-1$ at $z\lesssim0.5$ and $w(z)>0$ at $z\gtrsim1$. Its properties at best fit are shown in Fig. 3. The values of the best fit parameters are $a_1=-2.49\pm0.12$, $a_2=0.46\,^{+0.07}_{-0.05}$, and $a_3=0.33\pm0.06$. Compared to the quadratic ansatz of Ref. [40] this cubic ansatz has slightly better χ^2_{min} and $w(z)$ is larger than the corresponding $w(z)$ of the quadratic ansatz at $z>1$ shown in Ref. [40] and in Fig. 3.

(2) Linder [41] ansatz $w(z)=w_0+w_1z/(1+z)$ (LA):

$$H^2(z)=H_0^2[\Omega_{0m}(1+z)^3$$
$$+(1-\Omega_{0m})(1+z)^{3(1+w_0+w_1)}e^{3w_1(1/1+z-1)}].$$
$$(2.21)$$

It can easily be verified using Eq. (2.18) that the ansatz (2.21) leads to a $w(z)$ of the form

$$w(z)=w_0+\frac{w_1z}{1+z}. \qquad (2.22)$$

This ansatz was suggested by Linder [41] and it is designed to interpolate between two values of w: $w(z)=w_0$ at $z\simeq0$ and $w(z)\simeq w_1$ at $z\gg1$. It does not give a very good fit (compared to other two parameter ansatze) to the data ($\chi^2_{min}=197.1$), even though it is still better than LCDM. The rea-

son is that it only allows a slow change of $w(z)$ with redshift between w_0 and w_1 while the data seem to require a more "abrupt" change from w_0 to w_1 at $z\simeq0.5$. The best fit values of these parameters are $w_0=-1.18\pm0.10$, $w_1=2.79\pm0.05$, and $\Omega_{0m}=0.24$.

(3) Linear ansatz $w(z)=w_0+w_1z$:

$$H^2(z)=H_0^2[\Omega_{0m}(1+z)^3$$
$$+(1-\Omega_{0m})(1+z)^{3(1+w_0-w_1)}e^{3w_1z}]. \quad (2.23)$$

This ansatz was suggested in Refs. [42–44] in a more general power series form. It can give very good fits for low redshift data ($z\lesssim0.5$) but it cannot fit well the general form of $w(z)$ at $z\gtrsim1$. At best fit it gives $\chi^2_{min}=196.4$, for $\Omega_{0m}=0.24$, which is about average compared to the other ansatze. The best fit parameter values are $w_0=-1.13\pm0.09$ and $w_1=1.86^{+0.08}_{-0.01}$, which leads to $w(z)>0.5$ for $z\gtrsim1$.

(4) Chaplygin Gas (CG) and Generalized Chaplygin Gas (GCG) [9,45–56]:

$$H^2(z)=H_0^2[\Omega_{0m}(1+z)^3+(1-\Omega_{0m})\sqrt{A+(1-A)(1+z)^\alpha}],$$
$$(2.24)$$

where the above form of $H(z)$ is a generalization of the usual Chaplygin gas ansatz which is obtained for $\alpha=6$ [46]. For $\alpha=6$ the equation of state of Chaplygin gas dark energy is

$$p_c=-\frac{A}{\rho_c}. \qquad (2.25)$$

From the form of Eq. (2.24) it is clear that the Chaplygin gas behaves like pressureless dust at high redshifts and like a cosmological constant at $z \simeq 0$. The sound velocity of Chaplygin gas grows rapidly and approaches the velocity of light at late redshifts ($v_s = \sqrt{dp_c/d\rho_c} = \sqrt{A}/\rho_c \sim t^2$). Thus inhomogeneities of Chaplygin gas do not grow (since the Jeans length approaches the horizon) and no constraints can be imposed from large scale structure observations. The physical motivation of the Chaplygin gas equation of state (2.25) comes from string theories [57]. In fact, considering a d brane in a $d+2$ dimensional space-time, the introduction of light cone variables in the resulting Nambu-Goto action leads to the action of a Newtonian fluid with equation of state (2.25).

The limitation of the Chaplygin gas ansatz is that it constrains $w(z)$ to $w(z) < 0$ at all finite redshifts. Thus its goodness of fit is below average ($\chi^2_{min} = 197.4$ for $\Omega_{0m} = 0.24$ and $A = 0.92 \pm 0.03$). This limitation does not exist for the generalized Chaplygin gas ansatz (arbitrary α) which gives a much better fit ($\chi^2_{min} = 194.8$ for $\Omega_{0m} = 0.24$ and $A = 0.9966^{+0.0001}_{-0.0004}, \alpha = 13.75^{+0.02}_{-0.04}$). This fit gives $w(z) \simeq 1.2 > 0$ for $z \gtrsim 1$ (see Fig. 3) as do all the ansatze with above average goodness of fit.

(5) Generalized Cardassian ansatz (CA):

$$H^2(z) = H_0^2[\Omega_{0m}(1+z)^3 + (1-\Omega_{0m})f_X(z)], \quad (2.26)$$

where

$$f_X(z) = \frac{\Omega_{0m}}{1-\Omega_{0m}}(1+z)^3\left[\left(1 + \frac{\Omega_{0m}^{-q}-1}{(1+z)^{3(1-n)q}}\right)^{1/q} - 1\right]. \quad (2.27)$$

This model [58,59] emerges from a generalization of the Friedman equations and predicts accelerated expansion at recent times without any dark energy. In this model the universe is flat and consists only of matter and radiation. Here we follow Ref. [58] and consider the generalization (2.27) of the original Cardassian ansatz of Ref. [10]. The original ansatz is obtained from Eq. (2.27) by setting $q=1$ and is equivalent to quiessence ($w = $ const). The generalized Cardassian ansatz has been fitted to SnIa data in Ref. [58] using a much smaller SnIa dataset with redshifts $z < 1$. We find (see Table I) that this ansatz gives a relatively poor fit to the data ($\chi^2_{min} = 198.3$ for $\Omega_{0m} = 0.34$ and $q = 0.045^{+0.008}_{-0.010}$, $n = -15^{+8}_{-9}$) below the average goodness of fit for the models considered and only slightly better compared to LCDM with $\Omega_{0m} = 0.34$ ($\chi^2_{min} = 198.7$). The predicted $w(z)$ increases with z but remains negative (see Fig. 3).

(6) Generalized Quardatic ansatz (GQuad):

$$H^2(z) = H_0^2[\Omega_{0m}(1+z)^3 + a_1(1+z)^{3(1+w_1)}$$
$$+ a_2(1+z)^{3(1+w_2)} + (1-a_1-a_2-\Omega_{0m})]. \quad (2.28)$$

This is another generalization of the quadratic polynomial fit for $H(z)$ of Ref. [40]. Here we do not add an arbitrary cubic term. Instead we allow the exponents of the two monomials

to vary and minimize with respect to the four parameters a_1, a_2, w_1 and w_2 instead of two parameters a_1 and a_2 with fixed $w_1 = -2/3$ and $w_2 = -1/3$ for the quadratic model. The fit of the generalized ansatz is better ($\chi^2_{min} = 195.1$ for $\Omega_{0m} = 0.24$ and $a_1 = -0.06^{+0.03}_{-0.02}$, $a_2 = 4^{+0.3}_{-0.2}10^{-3}$, $w_1 = -1.13 \pm 0.24$, and $w_2 = 2.42 \pm 0.02$) than the quadratic ansatz ($\chi^2_{min} = 196.8$ for $\Omega_{0m} = 0.34$, $a_1 = -3.85^{+1.16}_{-1.27}$, and $a_2 = 1.63^{+0.79}_{-0.63}$) and the best fit form of $w(z)$ differs significantly from the corresponding quadratic best fit particularly for $z \gtrsim 1$. In particular we find that $w(z) \simeq -1$ for $z \lesssim 0.4$ and $w(z) \gtrsim 2$ for $z \gtrsim 1$. For comparison the quadratic ansatz of Ref. [40] predicts $w(z) \simeq 0$ for $z \gtrsim 1$ with very small 2σ errors at $z > 1$. This disagreement of our generalized ansatz with the quadratic ansatz at $z > 1$ despite the small 2σ error regions is another indication of the limited usefulness of ploting 1σ and 2σ error regions of $w(z)$ in the context of a particular ansatz. These regions can be easily violated in the context of another ansatz with better or similar fit.

A variant of this ansatz is one where one of the two arbitrary power law terms is replaced by an exponentially increasing term. The corresponding ansatz ($\sinh + DE$) is

$$H^2(z) = H_0^2[\Omega_{0m}(1+z)^3 + a_1(1+z)^{3(1+w_1)} + a_2\sinh(w_2 z)$$
$$+ (1-a_1-\Omega_{0m})]. \quad (2.29)$$

The results for this ansatz are almost identical to those of Eq. (2.28) (see Table I and Fig. 3).

(7) Oscillating ansatz (OA):

$$H^2(z) = H_0^2[\Omega_{0m}(1+z)^3 + a_1\cos(a_2 z^2 + a_3)$$
$$+ (1-a_1\cos(a_3) - \Omega_{0m})]. \quad (2.30)$$

This is our best fit ansatz. It gives a better fit to the data than any of the other ansatze ($\chi^2_{min} = 193.8$ for $\Omega_{0m} = 0.34$, $a_1 = -3.22^{+0.93}_{-0.76}$, $a_2 = 2.28^{+0.93}_{-0.76}$, and $a_3 = -0.08\pi \pm 0.01\pi$). The behavior of $w(z)$, however, for $z \gtrsim 1$ is qualitatively different compared to the other ansatze (see Fig. 3). For $z \lesssim 0.3$ we find $w(z) \simeq -1$. For $0.5 \lesssim z \lesssim 1.2$ we find $w(z) > 0$ with a maximum $w(z \simeq 0.75) \simeq 1.5$. At $z \gtrsim 1.2$, $w(z)$ becomes negative and continues oscillating around $w \simeq 0$ with large amplitude. This redshift range, however, includes only one data point at $z = 1.75$, which cannot constrain the behavior of $w(z)$ and $H(z)$ in any statistically significant way.

The quality of the fit for the oscillating ansatz combined with indications from the better fits of other ansatze that indicate $w(z) > 0$ for $z \gtrsim 1$ supports the idea that some type of oscillation probably takes place for $w(z)$.

From the theoretical viewpoint this idea is also supported for two reasons:

(a) *Coincidence problem resolution*: An oscillating expansion rate can help resolve the coincidence problem since our present accelerating phase is viewed simply as part of a sequence of accelerating and decelerating periods in the expansion history of the Universe [31,32].

(b) *Extra dimensions:* Models with extra dimensions generically predict oscillations of the stabilized modulus of the extra dimension size (the radion field) due to its coupling to

redshifting matter [11,12]. These oscillations backreact on the expansion rate and induce oscillations of the Hubble parameter.

Another factor pointing towards oscillating expansion rate is the north-south pencil beam survey of Ref. [60], which suggests an apparent periodicity in the galaxy distribution. The number of galaxies as a function of redshift seems to clump at regularly spaced intervals of $128h^{-1}$ Mpc. Recent simulations [61] have indicated that this regularity has a priori probability less than 10^{-3} in CDM universes with or without a cosmological constant. An oscillating expansion rate could resolve this puzzle without invoking special features in the primordial fluctuations spectrum.

III. CONCLUSION

We have fitted several cosmological models using the maximum likelihood method and the most recent SnIa data consisting of 194 data points. No priors have been used in our analysis other than those indicated by other observations, i.e., flatness and $\Omega_{0m} = 0.29 \pm 0.05$.

We have confirmed recent studies [40,62,63] indicating an increase of the equation of state parameter with redshift termed metamorphosis of dark energy in a recent study [40]. We have shown, however, that the best fit ansatze indicate that this metamorphosis continues beyond $w(z) = 0$ and leads to $w(z) > 0$ at $z \simeq 1$. Nucleosynthesis and large scale structure constraints are not consistent with $w(z) > 0$ at arbitrarily high redshifts. Thus our best fits to the data can only be made consistent with these constraints if some kind of oscillating behavior is realized for the effective dark energy equation of state parameter $w(z)$. This possibility is further enhanced by the fact that an oscillating expansion rate ansatz has provided the best fit to the data among all the 13 ansatze considered and also by other theoretical and observational arguments discussed in the previous section.

At low redshifts ($z < 0.5$) all the fitted ansatze approach $w(z) \simeq -1$ with $w(z)$ approximately constant. Most (but not all) of the better fits predict $w(z)$ slightly less than -1 (up to -1.3) for some redshift range within $[0,0.5]$ but not necessarily at $z = 0$. There are good fits, however (like the *quiessence*-Λ ansatz), with χ^2_{min} below average for which $w(z) > -1$ for all z implying that phantom energy [64,65] ($w < -1$) is consistent with the data but is not necessarily more probable than dark energy ($w > -1$). Since there are good fits with $w(z) > -1$ and rapidly increasing $w(z)$ for $z > 0.5$, we conclude that even if the prior $w > -1$ were used, with the proper ansatz we would still be able to see the rapid increase of $w(z)$ with z. This does not agree with the conclusion of Ref. [40] that it is the use of priors that would hide the increase of $w(z)$ with redshift. Here we have shown that the cosmological ansatz selection can also play a crucial role in revealing or hiding the true expansion history of the universe. Other comparisons of particular ansatze with the SnIa data can also be found in the literature [66–70].

Thus we are led to an important question: *Is there a systematic way to use the SnIa data in constructing a relatively simple cosmological ansatz that will give the best possible fit to the data given the number of parameters?* Addressing this important issue will be the subject of a subsequent paper.

APPENDIX

Here we demonstrate that the marginalization over the zero point magnitude $\bar{M}$ defined in Eq. (1.6) would have negligible effect $[O(1\%)]$ on our results. Any model will predict the theoretical value $D_L^{th}(z;a_1, \ldots, a_n)$ with some undetermined parameters a_i (e.g., Ω_m, Ω_Λ). The best-fit model is obtained by minimizing the quantity [18]:

$$\chi^2(\bar{M}') = \sum_{i=1}^{N} \frac{[\log_{10}D_L^{obs}(z_i) - 0.2\bar{M}' - \log_{10}D_L^{th}(z_i)]^2}{(\sigma_{\log_{10}D_L(z_i)})^2 + \left(\frac{\partial \log_{10}D_L(z_i)}{\partial z_i}\sigma_{z_i}\right)^2},$$

(A1)

where $\bar{M}' = \bar{M} - \bar{M}_{obs}$ is a free parameter representing the difference between the actual $\bar{M}$ [see Eq. (1.6)], and its assumed value $\bar{M}_{obs}$ in the data.

Uniform marginalization over $\bar{M}'$ corresponds to integrating over $\bar{M}'$ and therefore working with a $\bar{\chi}^2$ defined by

$$\bar{\chi}^2 = -2\ln\left(\int_{-\infty}^{+\infty} e^{-\chi^2/2}d\bar{M}'\right),$$

(A2)

which after some manipulation gives

$$\bar{\chi}^2 = -2\ln\left(\int_{-\infty}^{+\infty} e^{-(1/2)C\bar{M}'^2 + B\bar{M}' - A/2}d\bar{M}'\right),$$

(A3)

where

$$A = \sum_{i=1}^{N} \frac{a_i^2}{\sigma_i^2} = \chi^2(\bar{M}' = 0), \quad B = 0.2\sum_{i=1}^{N} \frac{a_i}{\sigma_i^2}$$

(A4)

and

$$C = 0.04\sum_{i=1}^{N} \frac{1}{\sigma_i^2}$$

(A5)

with

$$a_i = \log_{10}D_L^{data} - \log_{10}D_L^{th}.$$

(A6)

Thus, the "marginalized" over $\bar{M}'$ χ^2 is

$$\bar{\chi}^2 = \chi^2(\bar{M}' = 0) - \frac{B^2}{C} + \ln\left(\frac{C}{2\pi}\right) \simeq \chi^2(\bar{M}' = 0)$$

(A7)

because in the cases considered the last two terms on the right-hand side of Eq. (A7) are of $O(1)$ while the first is $O(10^2)$ and therefore dominates over the others. Thus the effects of the marginalization are of order 1% and can be neglected. This same conclusion has also been reached in Ref. [25].

---

[1] Supernova Search Team Collaboration, A.G. Riess *et al.*, Astron. J. **116**, 1009 (1998); Supernova Cosmology Project Collaboration, S. Perlmutter *et al.*, Astrophys. J. **517**, 565 (1999).

[2] V. Sahni, astro-ph/0403324.

[3] V. Sahni and A.A. Starobinsky, Int. J. Mod. Phys. D **9**, 373 (2000).

[4] P.J. Peebles and B. Ratra, Astrophys. J. Lett. **325**, L17 (1988); R.R. Caldwell, R. Dave, and P.J. Steinhardt, Phys. Rev. Lett. **80**, 1582 (1998); I. Zlatev, L.M. Wang, and P.J. Steinhardt, *ibid.* **82**, 896 (1999).

[5] V. Sahni and L.M. Wang, Phys. Rev. D **62**, 103517 (2000).

[6] F. Perrotta, C. Baccigalupi, and S. Matarrese, Phys. Rev. D **61**, 023507 (2000); A. Riazuelo and J.P. Uzan, *ibid.* **66**, 023525 (2002); G. Esposito-Farese and D. Polarski, *ibid.* **63**, 063504 (2001).

[7] D.F. Torres, Phys. Rev. D **66**, 043522 (2002).

[8] S. Nojiri and S.D. Odintsov, Gen. Relativ. Gravit. **36**, 1765 (2004).

[9] A.Y. Kamenshchik, U. Moschella, and V. Pasquier, Phys. Lett. B **511**, 265 (2001).

[10] K. Freese and M. Lewis, Phys. Lett. B **540**, 1 (2002).

[11] L. Perivolaropoulos and C. Sourdis, Phys. Rev. D **66**, 084018 (2002).

[12] L. Perivolaropoulos, Phys. Rev. D **67**, 123516 (2003).

[13] V. Sahni and Y. Shtanov, J. Cosmol. Astropart. Phys. **0311**, 014 (2003).

[14] A.A. Starobinsky, Pis'ma Zh. Éksp. Teor. Fiz. **68**, 721 (1988) [JETP Lett. **68**, 757 (1998)].

[15] D. Huterer and M.S. Turner, Phys. Rev. D **64**, 123527 (2001).

[16] T. Chiba, N. Sugiyama, and T. Nakamura, Mon. Not. R. Astron. Soc. **301**, 72 (1998).

[17] W.H. Press *et al.*, *Numerical Recipes* (Cambridge University Press, Cambridge, 1994).

[18] T.R. Choudhury and T. Padmanabhan, Mon. Not. R. Astron. Soc. **344**, 823 (2003).

[19] Minuit, http://wwwinfo.cern.ch/asdoc/minuit/minmain.html (2002).

[20] NAG, http://anaphe.web.cern.ch/anaphe/gemini.html (2002).

[21] http://www.wolfram.com/

[22] L. Perivolaropoulos and S. Nesseris http://leandros.physics.uoi.gr/cosmofit.htm

[23] J.L. Tonry *et al.*, Astrophys. J. **594**, 1 (2003).

[24] B.J. Barris *et al.*, Astrophys. J. **602**, 571 (2004).

[25] E. Di Pietro and J.F. Claeskens, Mon. Not. R. Astron. Soc. **341**, 1299 (2003).

[26] P. de Bernardis *et al.*, Astrophys. J. **564**, 559 (2002).

[27] U. Alam, V. Sahni, T.D. Saini, and A.A. Starobinsky, Mon. Not. R. Astron. Soc. **344**, 1057 (2003).

[28] W.J. Percival *et al.*, Mon. Not. R. Astron. Soc. **327**, 1297 (2001).

[29] W. Freedman *et al.*, Astrophys. J. **553**, 47 (2001).

[30] T.D. Saini, S. Raychaudhury, V. Sahni, and A.A. Starobinsky, Phys. Rev. Lett. **85**, 1162 (2000).

[31] S. Dodelson, M. Kaplinghat, and E. Stewart, Phys. Rev. Lett. **85**, 5276 (2000).

[32] K. Griest, Phys. Rev. D **66**, 123501 (2002).

[33] U. Günther and A. Zhuk, Hadronic J. **21**, 279 (1998); U. Günther, S. Kriskiv, and A. Zhuk, Gravitation Cosmol. **4**, 1 (1998); U. Günther and A. Zhuk, Class. Quantum Grav. **15**, 2025 (1998); Phys. Rev. D **61**, 124001 (2000).

[34] U. Günther and A. Zhuk, Phys. Rev. D **56**, 6391 (1997).

[35] N. Arkani-Hamed, S. Dimopoulos, N. Kaloper, and J. March-Russell, Nucl. Phys. **B567**, 189 (2000); J.M. Cline, Phys. Rev. D **61**, 023513 (2000).

[36] I. Antoniadis, Phys. Lett. B **246**, 1990 (377).

[37] L. Randall and R. Sundrum, Phys. Rev. Lett. **83**, 4690 (1999); **83**, 3370 (1999).

[38] W.D. Goldberger and M.B. Wise, Phys. Rev. Lett. **83**, 4922 (1999).

[39] C. Csaki, M. Graesser, L. Randall, and J. Terning, Phys. Rev. D **62**, 045015 (2000); P. Kanti, I.I. Kogan, K.A. Olive, and M. Pospelov, *ibid.* **61**, 106004 (2000).

[40] U. Alam, V. Sahni, T.D. Saini, and A.A. Starobinsky, astro-ph/0311364.

[41] E.V. Linder, Phys. Rev. Lett. **90**, 091301 (2003).

[42] P. Astier, astro-ph/0008306.

[43] J. Weller and A. Albrecht, Phys. Rev. D **65**, 103512 (2002).

[44] I. Maor, R. Brustein, J. McMahon, and P.J. Steinhardt, Phys. Rev. D **65**, 123003 (2002).

[45] N. Bilic, G.B. Tupper, and R.D. Viollier, Phys. Lett. B **535**, 17 (2002).

[46] J.C. Fabris, S.V.B. Goncalves, and P.E.d. Souza, astro-ph/0207430.

[47] J.S. Alcaniz, D. Jain, and A. Dev, Phys. Rev. D **67**, 043514 (2003).

[48] P.P. Avelino, L.M.G. Beca, J.P.M. de Carvalho, and C.J.A. Martins, J. Cosmol. Astropart. Phys. **0309**, 002 (2003).

[49] L. Amendola, F. Finelli, C. Burigana, and D. Carturan, J. Cosmol. Astropart. Phys. **0307**, 005 (2003).

[50] M.C. Bento, O. Bertolami, and A.A. Sen, Phys. Rev. D **66**, 043507 (2002).

[51] M.C. Bento, O. Bertolami, and A.A. Sen, Gen. Relativ. Gravit. **35**, 2063 (2003).

[52] M.d.C. Bento, O. Bertolami, and A.A. Sen, Phys. Lett. B **575**, 172 (2003).

[53] P.T. Silva and O. Bertolami, Astrophys. J. **599**, 829 (2003).

[54] M.d.C. Bento, O. Bertolami, and A.A. Sen, Phys. Rev. D **67**, 063003 (2003).

[55] O. Bertolami, A.A. Sen, S. Sen, and P.T. Silva, Mon. Not. R. Astron. Soc. (to be published), astro-ph/0402387.

[56] V. Gorini, A. Kamenshchik, U. Moschella, and V. Pasquier, gr-qc/0403062.

[57] N. Ogawa, Phys. Rev. D **62**, 085023 (2000).

[58] Y. Wang, K. Freese, P. Gondolo, and M. Lewis, Astrophys. J. **594**, 25 (2003).

[59] Z.H. Zhu and M.K. Fujimoto, Astrophys. J. **585**, 52 (2003).

[60] T.J. Broadhurst, R.S. Ellis, D.C. Koo, and A.S. Szalay, Nature (London) **343**, 726 (1990).

[61] N. Yoshida *et al.*, Mon. Not. R. Astron. Soc. **325**, 803 (2001).

[62] Y. Wang and P. Mukherjee, ApJ **606**, 654 (2004).

[63] Y. Wang and K. Freese, astro-ph/0402208.

[64] R.R. Caldwell, Phys. Lett. B **545**, 23 (2002).

[65] R.R. Caldwell, M. Kamionkowski, and N.N. Weinberg, Phys. Rev. Lett. **91**, 071301 (2003).

[66] D. Carturan and F. Finelli, Phys. Rev. D **68**, 103501 (2003).

[67] Y.g. Gong and C.K. Duan, Mon. Not. R. Astron. Soc. 352, 847 (2004).

[68] Y.G. Gong and C.K. Duan, Class. Quantum Grav. **21**, 3655 (2004).

[69] J.M. Virey, P. Taxil, A. Tilquin, A. Ealet, D. Fouchez, and C. Tao, Phys. Rev. D **70**, 043514 (2004).

[70] Y.g. Gong and X.M. Chen, gr-qc/0402031.